Earthline Journal of Chemical Sciences
E-ISSN: 2581-9003; CODEN: EJCSB4
Volume 9, Number 2, 2023, Pages 249-265
https://doi.org/10.34198/ejcs.9223.249265

Diazoxide and its Tautomers - A DFT Treatment

Lemi Türker

Department of Chemistry, Middle East Technical University, Üniversiteler, Eskişehir Yolu No: 1, 06800 Çankaya/Ankara, Turkey; e-mail: lturker@gmail.com; lturker@metu.edu.tr

Abstract

Diazoxide have several potential effectors that may potentially contribute to cardio protection. It is used to manage symptoms of hypoglycemia that is caused by pancreas cancer, surgery, or other conditions. It also acts as a non-diuretic antihypertensive agent. Diazoxide possessing various tautomeric forms should display variable biological properties depending on its tautomer content. It may exhibit 1,3- and 1,5-type proton tautomerism. Presently, all those possible tautomeric forms are considered. All the calculations have been performed within the realm of density functional theory with the constraints of B3LYP/6-311++G(d,p) level. All the tautomers are electronically stable and thermo chemically favorable formation values at the standard conditions. Some quantum chemical and spectral properties of those tautomeric systems as well as nucleus-independent chemical shift (NICS) values have been obtained and discussed.

1. Introduction

Diazoxide structure (Figure 1), in the literature is given either as D1 (7-chloro-3-methyl-2H-1,2,4-benzothiacliazine-1,1-dioxide [1,2] or D2 (7-chloro-3-methyl-4*H*-1λ^6,2,4-benzothiadiazine 1,1-dioxide) [3]. They are indeed 1,3 tautomers. Diazoxide is a nondiuretic benzothiadiazine antihypertensive agent, attenuates vascular responses to a variety of vasoconstrictor substances [4]. It is chemically closely related to the thiazide diuretics lacks the 7-sulfonamide group and a halogen substitution at the 6-position. It does not inhibit carbonic anhydrase, and is devoid of chloriuretic and natriuretic activity. It is a potent and rapidly acting antihypertensive agent and, after 12 years of clinical trial, was marketed three years ago for intravenous therapy of hypertensive emergencies. Diazoxide exerts its hypotensive action entirely by reducing vascular resistance in all

Received: December 1, 2022; Accepted: January 3, 2023; Published: January 5, 2023

Keywords and phrases: diazoxide; thiazide diuretics; antihypertensive; tautomerism; NICS; DFT.

circulatory beds through direct relaxation of arteriolar smooth muscle. Investigations revealed that diazoxide competes with barium for a specific receptor site in the vascular smooth muscle of the rat aorta [4].

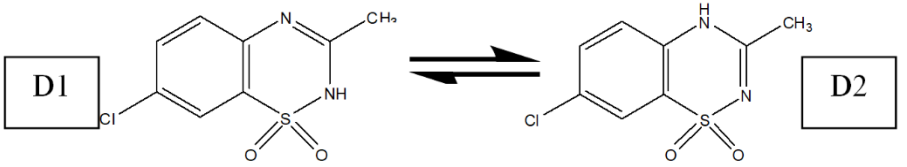

Figure 1. 2D-Structures for diazoxide.

Diazoxide causes hyperglycemia which can be inhibited by an adrenergic blocking agent and adrenalectomy. In adrenalectomized rats, noradrenaline has been shown to restore the hyperglycemic effect of diazoxide supported to a lesser extent by corticosteroids [5].

Through the years many articles have piled up in the literature about medicinal aspects of diazoxide [4-17]. In general, they point out that diazoxide may have several potential effectors that may potentially contribute to cardio protection, including K_{ATP} channels in the pancreas, smooth muscle, endothelium, neurons and the mitochondrial inner membrane. Diazoxide may also affect other ion channels and ATPases and may directly regulate mitochondrial energetics. It is possible that the success of diazoxide lies in this promiscuity and that the compound acts to rebalance multiple physiological processes during cardiac ischemia [18].

On the other hand, tautomers having different structures possess dual reactivity. Therefore, diazoxide which possesses various tautomeric forms should display variable biological properties (beside others) depending on its tautomer content (allelotropic mixture [19,20]). It is to be noted that substances which are isomeric under certain conditions are tautomeric under more drastic conditions [19,20].

Being the pioneers, Orita et al., interested in diazoxide molecule theoretically in 1970s and performed some Hückel's molecular-orbital calculations. However, since then only a few number of articles related to molecular orbital calculations or crystal structure of diazoxide have appeared in the literature [2,22]. Bandoli and Nicolini investigated the crystal and molecular structure of diazoxide in detail [22]. Quantum chemical calculations were employed by Kamal et al., to corroborate the observed experimental results for a series of derivatives [23]. For those compounds geometry optimization and frequency calculations were performed at B3LYP/6-31G(d) level. Furthermore, in order

to explain the reactivity of these molecules they calculated a gas-phase proton affinity (PA) values.

2. Method of Calculations

In the present study, all the initial geometry optimizations of the structures leading to energy minima have been achieved by using MM2 method then followed by semi-empirical PM3 self-consistent fields molecular orbital (SCF MO) method [24,25] at the restricted level [26]. Afterwards, the structure optimizations have been managed within the framework of Hartree-Fock (HF) and finally by using density functional theory (DFT) at the level of B3LYP/6-311++G(d,p) [27,28]. It is worth mentioning that the exchange term of B3LYP consists of hybrid Hartree-Fock and local spin density (LSD) exchange functions with Becke's gradient correlation to LSD exchange [29]. Also note that the correlation term of B3LYP consists of the Vosko, Wilk, Nusair (VWN3) local correlation functional [30] and Lee, Yang, Parr (LYP) correlation correction functional [31]. In the present study, the normal mode analysis for each structure yielded no imaginary frequencies for the 3*N*–6 vibrational degrees of freedom, where *N* is the number of atoms in the system. This search has indicated that the structure of each molecule corresponds to at least a local minimum on the potential energy surface. Furthermore, all the bond lengths have been thoroughly searched in order to find out whether any bond cleavage occurred or not during the geometry optimization process. All these computations were performed by using SPARTAN 06 [32]. Whereas the nucleus-independent chemical shift, NICS(0), calculations have been performed by using Gaussian 03 program [33].

3. Results and Discussion

Figure 2 shows the optimized structures of the tautomers of diazoxide. Direction of the calculated dipole moment vectors are also shown. Note that structure D1 and D2 are

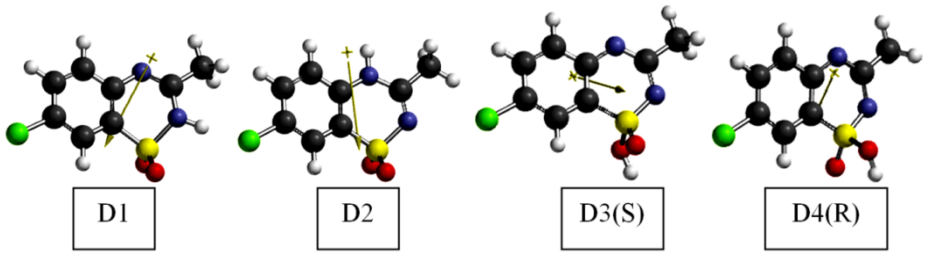

Figure 2. Optimized structures of the tautomers.

1,3-whereas the others are 1,5-type proton tautomers. Also note that presently considered 1,5-type tautomers are enantiomers of each other, namely the sulfur atom is a chiral center. Therefore they are label as D3(S) and D4(R). It has to be mentioned that direction of the dipole moment vectors in D3(S) and D4(R) are quite different from each other.

Figure 3 shows the calculated bond lengths of the tautomers considered. The C-S and N-S bonds in D1 and D2 are quite comparable whereas in D3(S) and D4(R) C-S bonds are longer than N-S bonds. Also in each enantiomeric tautomer S-O and S-OH bonds differ from each other. This should arise from the type of bonding involving the sulfur atom.

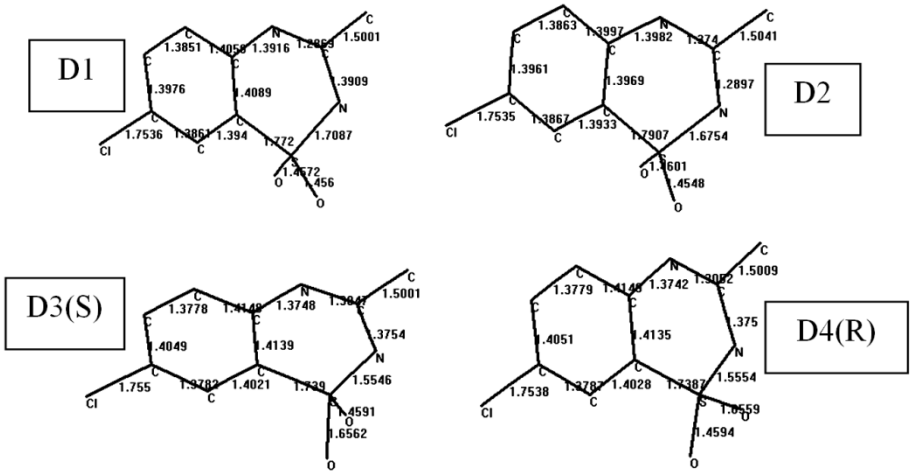

Figure 3. Calculated bond lengths of the tautomers considered (hydrogens not shown).

Figure 4 shows the calculated IR spectra of 1,3-tautomers of diazoxide. In the literature, as mentioned in the introduction part either of D1 or D2 is given as diazoxide formula. The N-H stretching in D1 occurs at 3564 cm^{-1} whereas in D2 it happens at 3615 cm^{-1}. In the cases of D3(S) and D4(R) O-H stretching occurs at 3749 cm^{-1} and 3750 cm^{-1}, respectively. Note that the enantiomeric tautomers D3(S) and D4(R) are 1,5-type tautomers and their occurrences are less likely than occurrences of 1,3-types, namely occurrences of D1 and D2.

The electrostatic potential (ESP) charges on atoms of the tautomers are depicted in Figure 5. Note that the ESP charges are obtained by the program based on a numerical method that generates charges that reproduce the electrostatic potential field from the entire wavefunction [32].

Figure 6 illustrates the electrostatic potential maps of the tautomers considered. The red/orange regions stand for negative whereas the blue regions for positive charge/ potential development. As seen in the figure the positive potential region in D2 spreads over much larger area compared to D1 case.

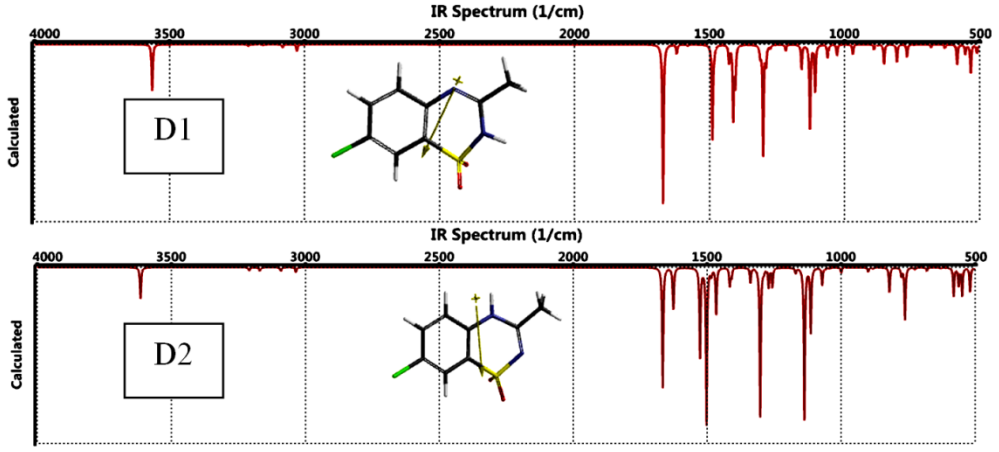

Figure 4. Calculated IR spectra of diazoxide and its 1,3-tautomer.

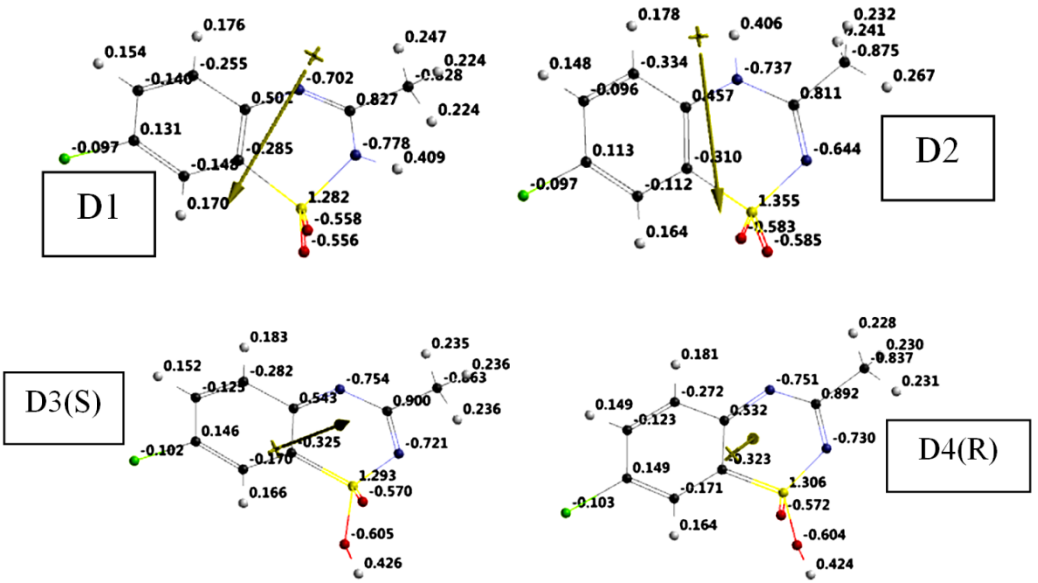

Figure 5. The electrostatic potential charges on atoms of the tautomers.

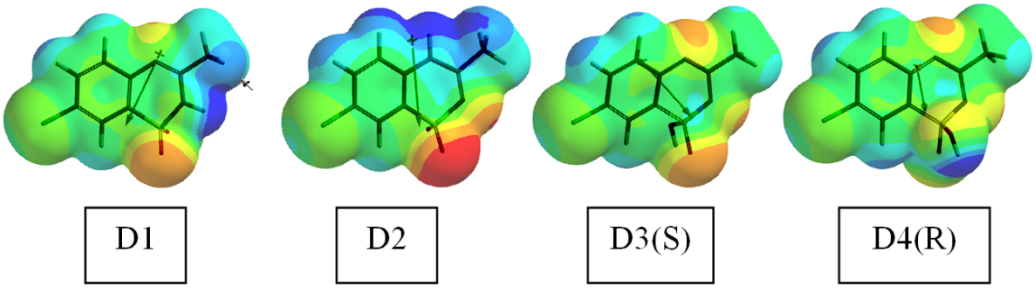

Figure 6. The electrostatic potential maps of the tautomers considered.

Table 1 tabulates some calculated properties of the tautomers considered. In the table the most striking property is that the dipole moments of 1,3-tautomers (D1 and D2) are much greater than the respective values of 1,5-tautomers. Also the value of D2 is much greater than the one of D1. This might arise from the comparative bond length differences (especially incident to the sulfur atom) and charges on atoms in D1 and D2. Components of the dipole moment vectors are listed in Table 2. In the cases of D1 and D2, Z-component of the vectors, in absolute value, is much greater than the other components. Whereas for the other tautomers considered, X-component of the vectors is greater than Y and Z-components. Note that components of the dipole moment vectors are not only the functions of charges and bond distances but also the angles with the coordinate axes, etc.

Table 1. Some calculated properties of the tautomers considered.

Tautomer	Dipole moment	Area (Å^2)	Volume (Å^3)	Ovality	Log P	Polarizability
D1	4.29	213.31	189.28	1.34	-1.43	55.57
D2	8.88	212.55	189.11	1.33	-1.13	55.49
D3(S)	1.42	213.83	189.38	1.34	-	55.61
D4(R)	1.42	213.83	189.38	1.34	-	55.61

Dipole moments in debye units. Polarizabilities in 10^{-30} m^3 units.

Table 2. Components of the dipole moment vectors.

Tautomer	X	Y	Z
D1	1.307120	-1.693101	-3.713932
D2	0.569051	0.981096	-8.810160
D3(S)	-1.227196	0.402304	-0.583786
D4(R)	1.221413	0.469462	-0.562147

In debye units.

As seen in Table 1 the ovality and polarizability values do not appreciably vary from one tautomer to other. On the other hand, the polarizability is defined according to the multi variable formula [32].

$$\text{Polarizability} = 0.08*V - 13.0353*h + 0.979920*h^2 + 41.3791$$

where V and h are the Van der Waals volume and hardness, respectively. Hardness is defined as,

$$\text{Hardness} = -(\varepsilon_{HOMO} - \varepsilon_{LUMO})/2$$

where ε_{HOMO} and ε_{LUMO} are the molecular orbital energies of the highest occupied (HOMO) and lowest unoccupied (LUMO) molecular orbital energies.

Table 3 shows some energies of the tautomers considered where E, ZPE and E_C stand for the total electronic energy, zero point vibrational energy and the corrected total electronic energy, respectively. The data reveal that all the structures considered are electronically stable. The stability order is D2>D1>D3(S)>D4(R). However keep in mind that the last two tautomers are enantiomeric.

Table 3. Some energies of the tautomers considered.

Tautomer	E	ZPE	E_C
D1	-3748017.42	381.53	-3747635.89
D2	-3748029.34	382.78	-3747646.56
D3(S)	-3747953.28	376.64	-3747576.64
D4(R)	-3747953.35	376.89	-3747576.46

Energies in kJ/mol.

Table 4 lists the calculated E(aq) values of the tautomers. The present calculations indicate that tautomer D2 is the preferred structure in vacuum as well as in aqueous conditions although in some of the literature D1 is presented as the structure of diazoxide.

Table 4. Calculated E(aq) values of the tautomers.

D1	D2	D3(S)	D4(R)
-3748090.13	-3748189.43	-3748048.93	-3748048.82

Energies in kJ/mol.

In Table 5 some thermo chemical values of the tautomers considered are tabulated. As seen in the table, all the structures have exothermic heat of formation and favorable Gibb's free energy of formation values at the standard state. The H^o and G^o values follow the order of D2<D1<D3(S)<D4(R).

Table 5. Some thermo chemical values of the tautomers considered.

Tautomer	H^o(kJ/mol.)	S^o (J/mol^o)	G^o(kJ/mol.)
D1	-3747639.355	429.89	-3747767.507
D2	-3747650.094	428.68	-3747777.904
D3(S)	-3747579.31	435.14	-3747709.037
D4(R)	-3747579.152	435.01	-3747708.853

Figure 7 displays some of the molecular orbital energy levels of the tautomers considered. Note that shift of proton from one nitrogen site to the other one, namely going from D1 to D2 highly perturbs the distribution of the inner lying molecular orbitals energy levels. The HOMO, LUMO energies and intermolecular orbital energy gap ($\Delta\varepsilon$) values of the tautomers are shown in Table 6. As seen in the table the HOMO and LUMO orders are D2<D1<D3(S)<D4(R) and D4(R)<D1<D3(S)<D2, respectively. So, D2 tautomer is characterized with the lowest HOMO and the highest LUMO values of all. These energy orders are reflected into the intermolecular orbital energy gap values, $\Delta\varepsilon$, ($\Delta\varepsilon=\varepsilon_{LUMO}-\varepsilon_{HOMO}$) that the order of $\Delta\varepsilon$ values happens as D2>D1>D3(S)>D4(R).

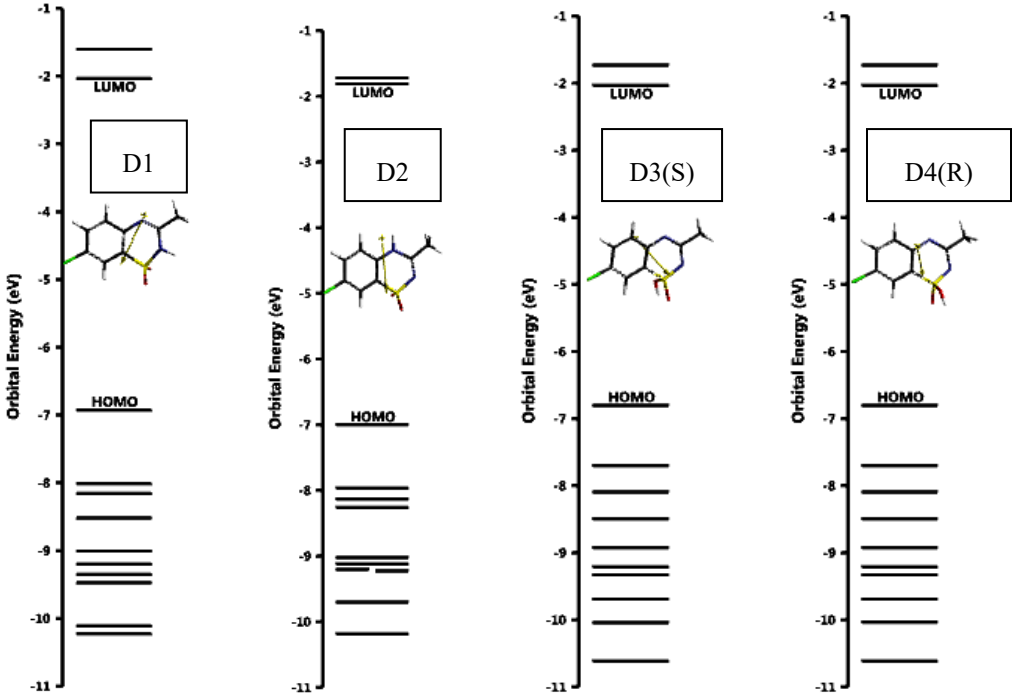

Figure 7. Some of the molecular orbital energy levels of the tautomers.

Table 6. The HOMO, LUMO energies and Δε values of the tautomers.

Tautomer	HOMO	LUMO	Δε
D1	-668.31	-195.88	472.43
D2	-675.72	-174.91	500.81
D3(S)	-656.36	-195.79	460.57
D4(R)	-656.30	-195.92	460.38

Energies in kJ/mol.

Figure 8 displays the HOMO and LUMO patterns of the tautomers considered. In general they exhibit π-type symmetry. In all the cases the methyl group supplies either nothing or very little to the HOMO and the LUMO. The same holds for the chlorine atom for the LUMOs.

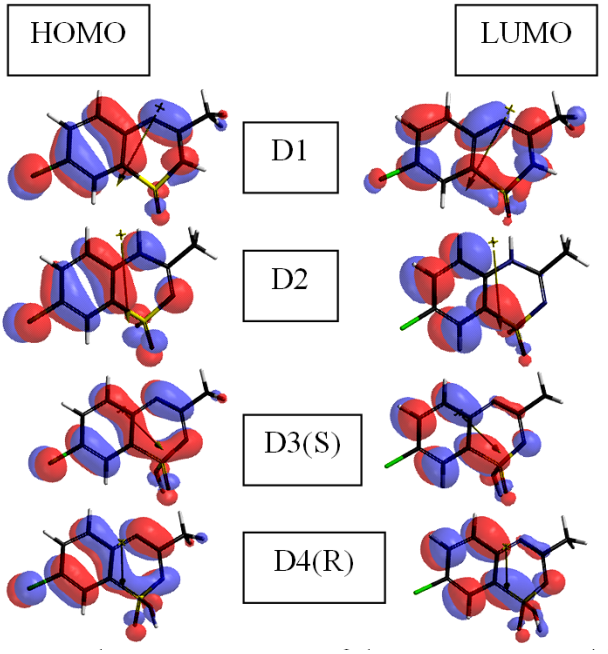

Figure 8. The HOMO and LUMO patterns of the tautomers considered.

Figure 9 shows the calculated UV-VIS spectra of the tautomers. The spectra lie in the ultraviolet region only. Except D2 spectrum, all the others have some discernable shoulders. The λ_{max} values are 259.17, 258.01, 261.40, 261.49 nm, respectively for D1 through D4(R). As compared to the order of $\Delta\varepsilon$ values, the quite big difference between $\Delta\varepsilon$ values of D1 and D2 has not been reflected to the order of λ_{max} values because in the calculated spectra not only the energies of the HOMO and LUMO orbitals but some others orbitals are involved as well.

Figure 10 is the local ionization potential map of diazoxide tautomers, where conventionally red/reddish regions (if any exists) on the density surface indicate areas from which electron removal is relatively easy, meaning that they are subject to electrophilic attack.

Figure 11 shows the LUMO maps of the diazoxide tautomers considered. Note that a LUMO map displays the absolute value of the LUMO on the electron density surface. The blue color (if any exists) stands for the maximum value of the LUMO and the red-colored region, associates with the minimum value. Various nucleophiles may attack on diazoxide, one of them is the hydride ion which causes ring opening reaction to produce some valuable compounds [34].

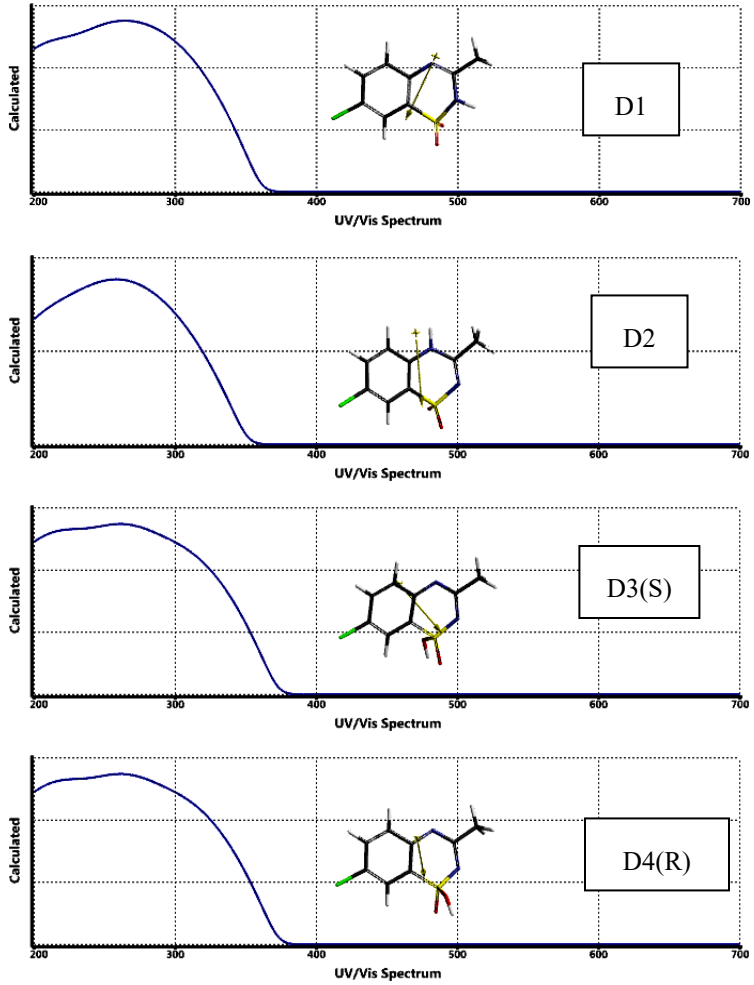

Figure 9. Calculated UV-VIS spectra of the tautomers.

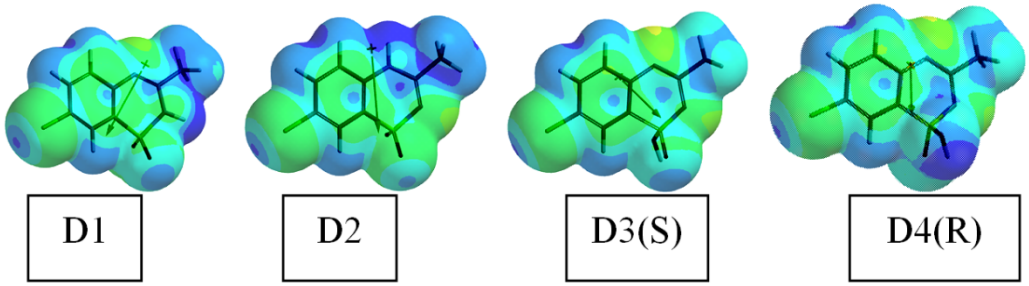

Figure 10. The local ionization maps of the tautomers.

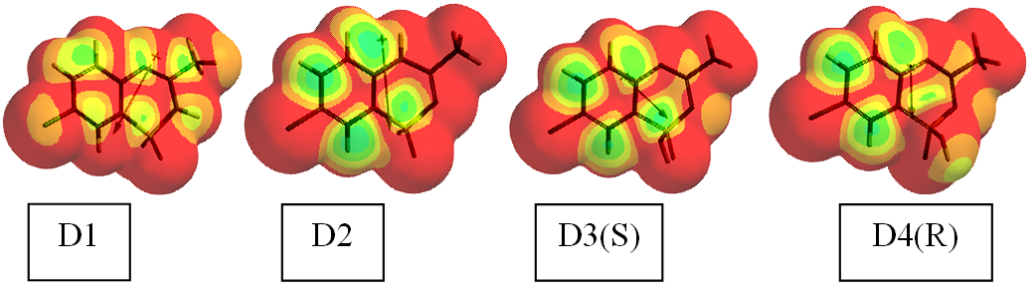

Figure 11. The LUMO maps of the tautomers.

NICS

To determine the local aromaticity of the rings present in the tautomers considered, "nucleus-independent chemical shift" (NICS) values were obtained. Note that NICS is the computed value of the negative magnetic shielding at some selected point in space, generally at center of a ring or cage. Through the years, theories developed on the subject and the calculated data so far have piled in the literature [35-46], have indicated that negative NICS values are associated with aromaticity (such as -11.5 for benzene, -11.4 for naphthalene). On the contrary, positive NICS values stand for antiaromaticity (28.8 for cyclobutadiene) while small NICS values are indicative of non-aromaticity (-2.1 for cyclohexane, -1.1 for adamantine). However, it is to be mentioned that although NICS approach has been proved to be an effective probe for the local aromaticity of individual rings of polycyclic systems a couple of contradictory results have been reported [46].

Table 7 shows the NICS(0) values for the presently considered tautomers of diazoxide. In the table the lower case letters, a and b, stand for the phenylene ring and the ring having the sulphone moiety, respectively. As seen in the table, a-ring of D2 is more aromatic than a-and b- rings of the other tautomers. The electron topology of D2 should have strengthen the ring current more favorably as compared to D1, thus the former one has a more aromatic a-ring. In the enantiomeric tautomers presently considered, a-rings have substantially more aromatic character than their b-rings which could fall into the non-aromatic classification. That should be due to the effect of SO(OH) moiety present in ring-b exerting some barrier to the ring current.

Table 7. The NICS(0) values of the tautomers considered.

D1a	D2a	D3a	D3b	D4a	D4b
-9.8304	-10.1836	-9.1792	-3.0033	-9.1764	-2.9771

4. Conclusion

The present DFT treatment at the level of B3LYP/6-311++G(d,p) has indicated (within the limitations of the theory and basis set) that in vacuum and aqueous conditions, diazoxide tautomers are electronically stable and have thermo chemically favorable formation values. Tautomer D1 is electronically less stable and thermo chemically less favorable compared to D2 although in some of articles in the literature, D1 is accepted as diazoxide structure. The phenylene ring in D2 is more aromatic than the respective ring of the other tautomers. So, a perturbation due to proton tautomerism occurring in b-ring affects NICS value of the adjacent ring in all the cases presently considered.

References

[1] Benowitz, N.L., & Bourne, H.R. (1984). Antihypertensive agents. In *Basic and clinical pharmacology*. (Katzung, B.G. Ed.). Los Altros, California: Lange Medical Pub.

[2] Orita, Y., Ando, A., Takamitsu, Y., Shirai, D., & Urakabe, S. (1972). Studies on Hückel's molecular orbital calculation (3d-2p) of the sulfamyl part of thiazide diuretics. *Jpn. Circ. J.*, *36*(2), 187-190. https://doi.org/10.1253/jcj.36.187

[3] Diazoxide, https://pubchem.ncbi.nlm.nih.gov

[4] Wohl, A.J., Hausler, L.M., & Roth, F.E. (1967). Studies on the mechanism of antihypertensive action of diazoxide: *in vitro* vascular pharmacodynamics. *Journal of Pharmacology and Experimental Therapeutics*, *158*(3), 531-539.

[5] Staquet, M., Yabo, R., & Wolff, J.F. (1965). An adrenergic mechanism for hyperglycemia induced by diazoxide, *Methabolism* (*Clinical and Experimental*), *14*(9), 1000-1009. https://doi.org/10.1016/0026-0495(65)90116-2

[6] Timlin, M., Black, A.B., Delaney, H.M., Matos, R.I., & Percival, C.S. (2017). Development of pulmonary hypertension during treatment with diazoxide: a case series and literature review. *Pediatr. Cardiol.*, *38*, 1247-1250. https://doi.org/10.1007/s00246-017-1652-3

[7] Anastacio, M.M., Kanter, E.M., Makepeace, C., Keith, A.D., Zhang, H., Schuessler, R.B., Nichols, C.G., & Lawton, J.S. (2013). Cardioprotective mechanism of diazoxide involves the inhibition of succinate dehydrogenase. *The Annals of Thoracic Surgery*, *95*(6), 2042-2050. https://doi.org/10.1016/j.athoracsur.2013.03.035

[8] Schäfer, G., Portenhauser, R., & Trolp, R. (1971). Inhibition of mitochondrial metabolism by the diabetogenic thiadiazine diazoxide—I: Action on succinate dehydrogenase and tca-cycle oxidations. *Biochemical Pharmacology*, *20*(6), 1271-1280. https://doi.org/10.1016/0006-2952(71)90358-3

[9] Sellitto, A.D., Maffit, S.K., Al-Dadah, A.S., Zhang, H., Schuessler, R.B., Nichols, C.G., & Lawton, J.S. (2010). Diazoxide maintenance of myocyte volume and contractility during stress: evidence for a non-sarcolemmal KATP channel location. *J. Thorac. Cardiovasc. Surg.*, *140*(5), 11531159. https://doi.org/10.1016/j.jtcvs.2010.07.047

[10] Mizutani, S., Al-Dadah, A.S., Bloch, J.B., Prasad, S.M., Diodato, M.D., Schuessler. R.B., Damiano, R.J., Jr., & Lawton, J.S. (2006). Hyperkalemic cardioplegia-induced myocyte swelling and contractile dysfunction: prevention by diazoxide. *Ann. Thorac. Surg.*, *81*(1), 154-9. https://doi.org/10.1016/j.athoracsur.2005.06.057

[11] Al-Dadah, A.S., Voeller, R.K., Schuessler, R.B., Damiano, R.J. Jr., & Lawton, J.S. (2007). Maintenance of myocyte volume homeostasis during stress by diazoxide is cardioprotective. *Ann. Thorac. Surg.*, *84*(3), 857-62. https://doi.org/10.1016/j.athoracsur.2007.04.103

[12] Maffit, S.K., Sellitto, A.D., Al-Dadah, A.S., Schuessler, R.B., Damiano, R.J. Jr., & Lawton, J.S. (2012). Diazoxide maintains human myocyte volume homeostasis during stress. *J. Am. Heart Assoc.*, *1*(2), e000778. https://doi.org/10.1161/jaha.112.000778

[13] Garlid, K.D., Paucek, P., Yarov-Yarovoy, V., Murray, H.N., Darbenzio, R.B., D'Alonzo, A.J., Lodge, N.J., Smith, M.A., & Grover, G.J. (1997). Cardioprotective effect of diazoxide and its interaction with mitochondrial ATP-sensitive K^+ channels. Possible mechanism of cardioprotection. *Circ. Res.*, *81*(6), 1072-82. https://doi.org/10.1161/01.res.81.6.1072

[14] Das, M., Parker, J.E., & Halestrap, A.P. (2003). Matrix volume measurements challenge the existence of diazoxide/glibenclamide-sensitive KATP channels in rat mitochondria. *J. Physiol.*, *547*(3), 893-902. https://doi.org/10.1113/jphysiol.2002.035006

[15] D'hahan, N., Moreau, C., Prost, A.L., Jacquet, H., Alekseev, A.E., Terzic, A., & Vivaudou, M. (1999). Pharmacological plasticity of cardiac ATP-sensitive potassium channels toward diazoxide revealed by ADP. *Proc. Natl. Acad. Sci.*, *96*(21), 12162-12167. https://doi.org/10.1073/pnas.96.21.12162

[16] Lim, K.H., Javadov, S.A., Das, M., Clarke, S.J., Suleiman, M., & Halestrap, A.P. (2002). The effects of ischaemic preconditioning, diazoxide and 5-hydroxydecanoate on rat heart mitochondrial volume and respiration. *J. Physiol.*, *545*(3), 961-974. https://doi.org/10.1113/jphysiol.2002.031484

[17] Graber, A.L., Porte, D. Jr., & Williams, R.H. (1966). Clinical use of diazoxide and mechanism for its hyperglycemic effects. *Diabetes*, *15*(3), 143-148. https://doi.org/10.2337/diab.15.3.143

[18] Coetzee, W.A. (2013). Multiplicity of effectors of the cardioprotective agent, diazoxide. *Pharmacol. Ther.*, *140*(2), 167-175. https://doi.org/10.1016/j.pharmthera.2013.06.007

[19] Reutov, O. (1970). *Theoretical principles of organic chemistry*, Moscow: Mir Pub.

[20] Anslyn, E.V., & Dougherty, D.A. (2006). *Modern physical organic chemistry*, Sausalito, California: University Science Books.

[21] Dupont, L., Pirotte, B., de Tullio, P., Masereel, B., & Delarge, J. (1995). Les activateurs de canaux potassiques: étude structurale comparative du pinacidil, du diazoxide et du cromakalim [Potassium channel activators: comparative structural study of pinacidil, diazoxide and cromakalim]. *Ann Pharm Fr*., *53*(5), 201-8. https://doi.org/10.1107/s0108767378095744

[22] Bandoli, G., & Nicolini, M. (1977). Crystal and molecular structure of diazoxide, an antihypertensive agent. *Journal of Crystal and Molecular Structure*, *7*, 229-240. https://doi.org/10.1007/BF01218380

[23] Kamal, A., Khan, M.N.A., Reddy, K.S., Rohini, K., Sastry, G.N., Sateesh, B., & Sridhar, B. (2007). Synthesis, structure analysis, and antibacterial activity of some novel 10-substituted 2-(4-piperidyl/phenyl)-5,5-dioxo[1,2,4]triazolo[1,5-b][1,2,4]benzothiadiazine derivatives. *Bioorganic & Medicinal Chemistry Letters*, *17*(19), 5400-5405. https://doi.org/10.1016/j.bmcl.2007.07.043

[24] Stewart, J.J.P. (1989). Optimization of parameters for semi empirical methods I. *J. Comput. Chem*., *10*, 209-220. https://doi.org/10.1002/jcc.540100208

[25] Stewart, J.J.P. (1989). Optimization of parameters for semi empirical methods II. *J. Comput. Chem*., *10*, 221-264. https://doi.org/10.1002/jcc.540100209

[26] Leach, A.R. (1997). *Molecular modeling*. Essex: Longman.

[27] Kohn, W., & Sham, L.J. (1965). Self-consistent equations including exchange and correlation effects. *Phys. Rev*., *140*, 1133-1138. https://doi.org/10.1103/PhysRev.140.A1133

[28] Parr, R.G., & Yang, W. (1989). *Density functional theory of atoms and molecules*. London: Oxford University Press.

[29] Becke, A.D. (1988). Density-functional exchange-energy approximation with correct asymptotic behavior. *Phys. Rev. A*, *38*, 3098-3100. https://doi.org/10.1103/PhysRevA.38.3098

[30] Vosko, S.H., Wilk, L., & Nusair, M. (1980). Accurate spin-dependent electron liquid correlation energies for local spin density calculations: a critical analysis. *Can. J. Phys.*, *58*, 1200-1211. https://doi.org/10.1139/p80-159

[31] Lee, C., Yang, W., & Parr, R.G. (1988). Development of the Colle-Salvetti correlation energy formula into a functional of the electron density. *Phys. Rev. B*, *37*, 785-789. https://doi.org/10.1103/PhysRevB. 37.785

[32] SPARTAN 06 (2006). Wavefunction Inc. Irvine CA, USA.

[33] Gaussian 03, Frisch, M.J., Trucks, G.W., Schlegel, H.B., Scuseria, G.E., Robb, M.A., Cheeseman, J.R., Montgomery, Jr., J.A., Vreven, T., Kudin, K.N., Burant, J.C., Millam, J.M., Iyengar, S.S., Tomasi, J., Barone, V., Mennucci, B., Cossi, M., Scalmani, G., Rega, N., Petersson, G.A., Nakatsuji, H., Hada, M., Ehara, M., Toyota, K., Fukuda, R., Hasegawa, J., Ishida, M., Nakajima, T., Honda, Y., Kitao, O., Nakai, H., Klene, M., Li, X., Knox, J.E., Hratchian, H.P., Cross, J.B., Bakken, V., Adamo, C., Jaramillo, J., Gomperts, R., Stratmann, R.E., Yazyev, O., Austin, A.J., Cammi, R., Pomelli, C., Ochterski, J.W., Ayala, P.Y., Morokuma, K., Voth, G.A., Salvador, P., Dannenberg, J.J., Zakrzewski, V.G., Dapprich, S., Daniels, A.D., Strain, M.C., Farkas, O., Malick, D.K., Rabuck, A.D., Raghavachari, K., Foresman, J.B., Ortiz, J.V., Cui, Q., Baboul, A.G., Clifford, S., Cioslowski, J., Stefanov, B.B., Liu, G., Liashenko, A., Piskorz, P., Komaromi, I., Martin, R.L., Fox, D.J., Keith, T., Al-Laham, M.A., Peng, C.Y., Nanayakkara, A., Challacombe, M., Gill, P.M.W., Johnson, B., Chen, W., Wong, M.W., Gonzalez, C., & Pople, J.A., Gaussian, Inc., Wallingford CT, 2004.

[34] Bouider, N., Fhayli, W., Ghandour, Z., Boyer, M., Harrouche, K., Florence, X., Pirotte, B., Lebrun, P., Faury, G., & Khelili, S. (2015). Design and synthesis of new potassium channel activators derived from the ring opening of diazoxide: Study of their vasodilatory effect, stimulation of elastin synthesis and inhibitory effect on insulin release. *Bioorganic and Medicinal Chemistry*, *23*, 1735-1746. http://doi.org/10.1016/j.bmc.2015.02.043

[35] Minkin, V.I., Glukhovtsev, M.N., & Simkin, B.Y. (1994). *Aromaticity and antiaromaticity: Electronic and structural aspects*. New York: Wiley.

[36] Schleyer, P.R., & Jiao, H. (1996). What is aromaticity?. *Pure Appl. Chem*., *68*, 209-218. https://doi.org/10.1351/pac199668020209

[37] Glukhovtsev, M.N. (1997). Aromaticity today: energetic and structural criteria. *J. Chem. Educ*., *74*, 132-136. https://doi.org/10.1021/ed074p132

[38] Krygowski, T.M., Cyranski, M.K., Czarnocki, Z., Hafelinger, G., & Katritzky, A.R. (2000). Aromaticity: a theoretical concept of immense practical importance. *Tetrahedron, 56*, 1783-1796. https://doi.org/10.1016/S0040-4020(99)00979-5

[39] Schleyer, P.R. (2001). Introduction: aromaticity. *Chem. Rev*., *101*, 1115-1118. https://doi.org/10.1021/cr0103221

[40] Cyranski, M.K., Krygowski, T.M., Katritzky, A.R., & Schleyer, P.R. (2002). To what extent can aromaticity be defined uniquely?. *J. Org. Chem*., *67*, 1333-1338. https://doi.org/10.1021/jo016255s

[41] Chen, Z., Wannere, C.S., Corminboeuf, C., Puchta, R., & Schleyer, P. von R. (2005). Nucleus independent chemical shifts (NICS) as an aromaticity criterion. *Chem. Rev.*, *105*(10), 3842-3888. https://doi.org/10.1021/cr030088

[42] Gershoni-Poranne, R., & Stanger, A. (2015). Magnetic criteria of aromaticity. *Chem. Soc. Rev*., *44*(18), 6597-6615. https://doi.org/10.1039/C5CS00114E

[43] Dickens, T.K., & Mallion, R.B. (2016). Topological ring-currents in conjugated systems. *MATCH Commun. Math. Comput. Chem*., *76*, 297-356.

[44] Stanger, A. (2010). Obtaining relative induced ring currents quantitatively from NICS. *J. Org. Chem*., *75*(7), 2281-2288. https://doi.org/10.1021/jo1000753

[45] Monajjemi, M., & Mohammadian, N.T. (2015). S-NICS: An aromaticity criterion for nano molecules. *J. Comput. Theor. Nanosci*., *12*(11), 4895-4914. https://doi.org/10.1166/jctn.2015.4458

[46] Schleyer, P.R., Maerker, C., Dransfeld, A., Jiao, H., & Hommes, N.J.R.E. (1996). Nucleus independent chemical shifts: a simple and efficient aromaticity probe. *J. Am. Chem. Soc*., *118*, 6317-6318. https://doi.org/10.1021/ja960582d